Available online at www.sciencedirect.com
SCIENCE DIRECT®
International Journal of Multiphase Flow 31 (2005) 179–200
International Journal of Multiphase Flow
www.elsevier.com/locate/ijmulflow

Fluctuating flow in a liquid layer and secondary spray created by an impacting spray

I.V. Roisman *, C. Tropea

Chair of Fluid Mechanics and Aerodynamics, Technical University of Darmstadt, Petersenstr. 30, 64287 Darmstadt, Germany

Received 9 September 2003; received in revised form 11 October 2004

Abstract

A spray impacting onto a wall produces a flow of secondary droplets. For relatively sparse spray these secondary droplets are produced by the splashing of the impacting drops and their interactions. For dense sprays, like Diesel injection sprays, these secondary droplets are created by the fluctuating liquid film created on the wall. In the present paper hydrodynamic models are presented for these two extreme cases. The velocities of the secondary droplets produced by the crown splash in a sparse spray are described theoretically. Next, the fluctuations in the motion of the liquid film created by a dense impacting spray are analyzed statistically. This motion yields the formation of finger-like jets, as observed in experiments of a Diesel spray impacting onto a rigid wall. The characteristic size and velocity of the film fluctuations are estimated. These two theoretical models are validated by comparison with the experimental data.

Keywords: Spray impact; Drop impact; Liquid film; Fluctuations; Jetting

* Corresponding author.
E-mail address: roisman@sla.tu-darmstadt.de (I.V. Roisman).

0301-9322/$ - see front matter © 2004 Elsevier Ltd. All rights reserved.
doi:10.1016/j.ijmultiphaseflow.2004.11.001

1. Introduction

A spray impacting onto a wall results in a fluctuating liquid layer. In some cases this layer breaks up and produces a stream of secondary droplets. This secondary stream can influence the charge mixture in combustion engines, the effectiveness of spray cooling, or the overall droplet population and size distribution in medical nebulizers. Further applications involve spray painting or spray deposition, for instance agricultural sprays.

The usual approach to the modelling of spray impact treats the phenomenon as a simple superposition of single drop impact events see (Stanton and Rutland, 1998; Mundo et al., 1998; Bai et al., 2002). Such models result from either experimental (Cossali et al., 1997; Rioboo et al., 2000) or theoretical (Yarin and Weiss, 1995) studies of the impact of a single drop onto a dry wall, onto a uniform, undisturbed liquid film or into a deep pool (Oğuz and Prosperetti, 1990).

Single impacting drop disturbs the liquid film on a substrate. If the impact velocity is small enough (below the splash threshold) the drop is simply deposited in the film and does not create any secondary drops. At higher impact velocities the impact creates an uprising sheet, bounded from above by a free rim formed due to capillary forces. When this rim is unstable, the bending deformations are followed by the formation of a number of small jets which then break up and create number of secondary droplets. These are the observed secondary droplets of the splash. In Fig. 1 various stages of such impact are shown.

This phenomenon is so fascinating that it is widely used in product advertisements. One empirical condition found for a crown splash is given in (Tropea and Roisman, 2000): $We^{4/5}Re^{2/5} \geqslant 2800$, valid for the case when the thickness of the film and the drop diameter are of the same order of magnitude.

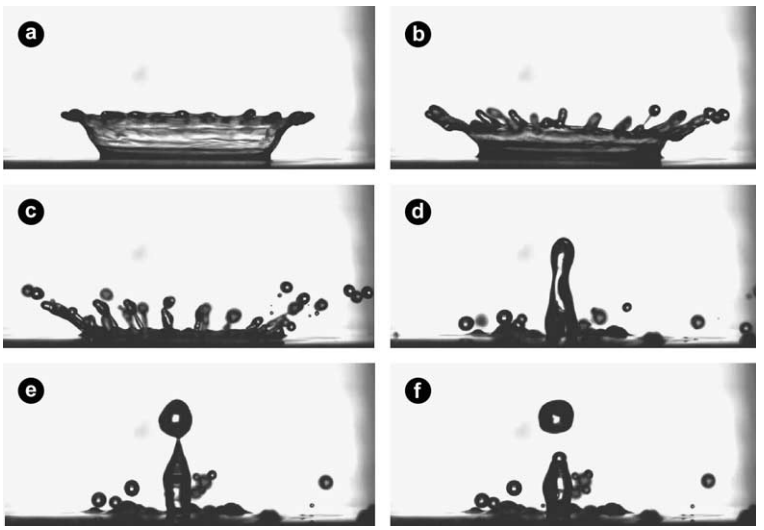

Fig. 1. Impact of a single drop onto a stationary liquid film leading to splash: (a) creation of a crown-like sheet; (b) formation of jets; (c) breakup of jets and creation of secondary droplets; (d) emerging of a central jet; (e) its deformation and (f) breakup.

If the thickness of the film is much larger than the drop diameter, the drop impact creates a crater in the liquid layer. When this crater recedes it can lead to bubble entrapment in the liquid and to the formation of an uprising central jet. Such impacts can also lead to splash when this central jet breaks up and creates a single or several secondary droplets. A condition for this central jet splash has been given by (Oğuz and Prosperetti, 1990) as: $We \geqslant 48.3\,Fr^{0.247}$.

The description of the phenomenon becomes much more complicated when the substrate is covered by wavy or even stationary but not uniform film. In Fig. 2 the normal impact of a single drop onto a flat partially wetted substrate is shown. The right side of the substrate is coated by a thin water layer. The left side is dry. The drop impacts at the edge of the liquid film. The uprising sheet created by the impact is not symmetrical, it is folded into a single, propagating to the right, tree-like jet. The outcome of such drop impact is obviously different from that of the impact onto a uniform liquid film.

Spray impact phenomenon is much more complicated than a simple superposition of single drop impacts. Images of a water spray in the neighborhood of the wall are shown in Fig. 3. The fluctuating liquid film created on the substrate, the uprising jets and secondary droplets can be clearly seen in the figure. The picture differs dramatically from the symmetric crown produced by single impact onto a stationary uniform film. In the experimental study of (Tropea and Roisman, 2000) the distributions of the drops and the mass flux densities of the spray before impact and after impact onto a target were measured and compared. The results were used to evaluate existing models of spray impact based on the superposition principle. It was shown that this conventional approach to modelling is not universal in the description of the spray impact, particularly, these models are not able to predict correctly the volume flux density vector of the secondary spray. In the case of relatively dense sprays, the interaction of crowns and the fluctuations of the liquid-wall film must be taken into account (Sivakumar and Tropea, 2002).

In Fig. 4 two different results of water spray impact are shown. In the first case (Fig. 4(a)) the intensity of the spray is relatively low, the droplets from the spray mostly deposit on the target surface and are collected in drops formed on the sphere due to the wettability effects and move along the surface under the effect of gravity. The second image (Fig. 4(b)) corresponds to a higher

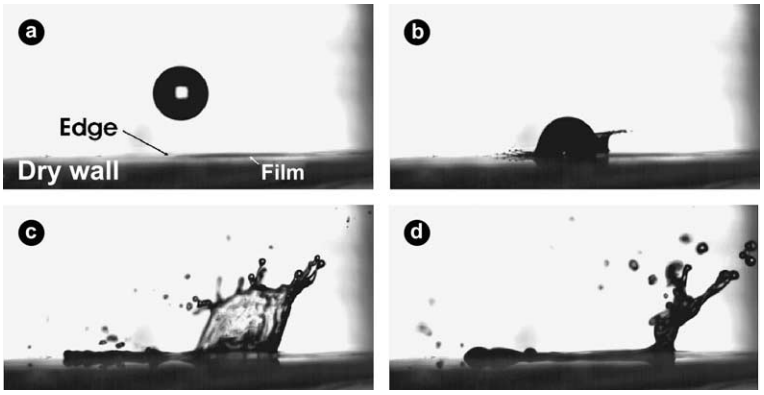

Fig. 2. Time sequence of an impact of a single drop onto a flat wall at the edge of a stationary liquid film. The left side of the wall surface is initially dry, whereas the right side is wetted.

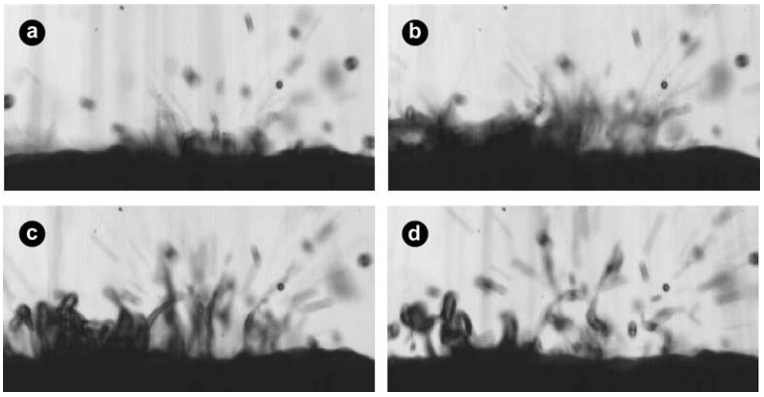

Fig. 3. Sequence of impact of a spray onto a flat rigid wall. Almost vertical thin lines correspond to the primary drops impacting with the relatively high velocity. Spherical drops are the low-speed secondary droplets.

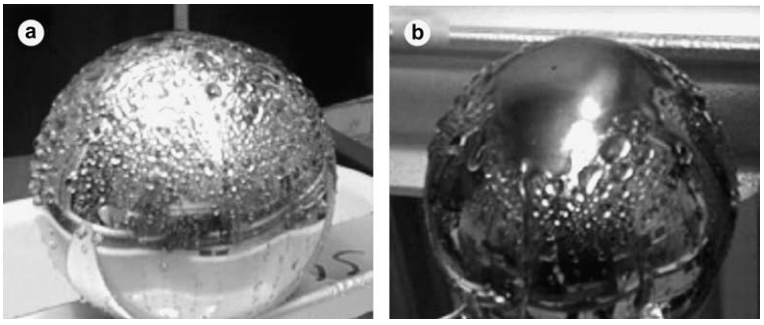

Fig. 4. Liquid layer formed on a surface of a spherical target by impact of a water spray of different intensities: (a) The deposited spray liquid coalesces into drops flowing down the target surface and (b) a thin liquid film is created by the spray.

spray intensity (higher total flux, droplet average velocity). In this case a relatively thin continuous liquid film appears on the sphere. In Fig. 5 the impact of a Diesel spray onto an inclined, cylindrical target is shown. In this picture the spray impact results in the creation of numerous uprising finger-like jets on the wall. Measurements performed using the phase Doppler technique indicate that secondary droplets are ejected from the wall. The average drop diameter in the impinging spray was $D \sim 10$ μm, the impact velocity $U \sim 40$ m/s, and the volume flux density approximately $\dot{q} \sim 0.1$ m/s. The resulting impact parameters fall far below either of the above-mentioned splash conditions. The image in Fig. 5 is obtained using the SensiCam CCD camera with an exposure time of 0.1 ms. As a result the primary drops moving with a relatively high velocity are observed as streaks. The velocity of the jet stretching is not estimated from the image. However, these jets are not straight and slightly curved. Therefore, we assume that these images correspond to the jets (as in Fig. 3) and not to high-speed secondary or primary drops.

It is known that the flows in the film produced by spray or drop impact, and all the corresponding phenomena, such as jetting, splash, *etc.* are inertia dominated. The model of single drop impact in

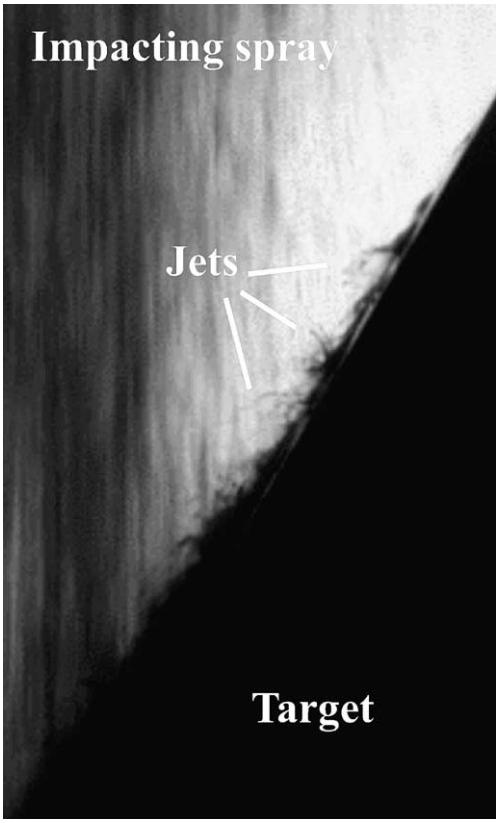

Fig. 5. Image of the diesel spray impacting onto an inclined target. The uprising finger-like jets can be clearly seen. The shape of the dry target has been superimposed onto the image.

(Roisman et al., 2002b) neglects the effect of the air drag completely, and the theory of (Yarin and Weiss, 1995) neglect even the effect of capillary forces and viscosity. These models nevertheless successfully predict the features of impact. These results indicate that effects such as the Kelvin–Helmholtz instability associated with the gas flow, capillary waves, short compressible shock waves during drop impact etc. are secondary and do not play any significant role in the phenomena.

Furthermore, the motion of the film and its fluctuations appear to influence significantly the drop impact process and apparently can enhance the splash, compared with single drop impacts. For instance (Sivakumar and Tropea, 2002) observe lower crowns with shorter lifetimes on films under sprays.

It is obvious, that the liquid film flow on the target surface in the cases shown in Figs. 4(a) and (b) and 5 are very different and thus, the transport in such flows and the break-up of the films must be modelled differently. Presently there is no theory able to predict quantitatively the regions of validity of such modes of film flows. It is clear that the inertia of flow fluctuations play a significant role in such flows, but also the wettability of the surface may be important.

The modelling of spray impact can be subdivided into four main parts. The first is the description of a spray, including the definition of the main parameters characterizing spray transport. The second part is the description of the boundary conditions at the spray/liquid interface. The

third part, which is one of the subjects of the present paper, is the description of the dynamics of the flow of the liquid layer. The analysis of fluctuations of this flow is of importance in the fourth part; the description of the flux and distribution of secondary droplets obtained by the atomization of the liquid layer by spray impact.

The conditions at which drops of the spray impact onto a fluctuating film on the wall differ from those of a single drop impact onto a stationary, uniform film. The volume flux of the liquid from the spray creates an average flow in the film parallel to the wall. This means that even if the drop velocity is normal to the wall, the impact is in fact not axisymmetric but locally oblique. Also the wavy surface of the liquid film may have some influence on the impact. Next, the fluctuations in the film have a vanishing time-averaged volume flux but non-zero momentum. The inertial terms associated with the fluctuations of the flow can affect the temporal evolution of the crown and thus, the velocity vector of the secondary droplets after splash. The fluctuations in the film can increase the amplitude of the perturbations in the crown affecting the splash threshold. The outcome of the drop impact can be influenced by direct interactions with another crown (or even crowns). Presently, there is definitely a lack of experimental data and a lack of understanding of these processes characteristic for the spray impact phenomena.

In the present paper the film motion caused by the impact of a single drop, formation of the uprising jet, as well as the velocities of secondary droplets produced by splash are analyzed in Section 2. The splashing threshold, the drop diameter distributions and the influence of the film fluctuations on these parameters are not considered in the present paper. A theoretical model for the velocities of the secondary drops produced by a single drop impact onto a stationary uniform film is applied to the description of spray impact. These results are applicable to the case of sparse sprays where the effect of the film fluctuations on the drop impact is not significant and the probability of direct interactions of the drops on the wall is small.

The hydrodynamics of impact of relatively dense sprays, influenced considerably by the film fluctuations and interactions of drops, is not yet studied in detail. Particularly, the following problems are not yet solved or even considered in the literature:

- magnitudes for typical film velocities or, frequency of the film fluctuations produced by drop impacts;
- characteristic length scale of these fluctuations;
- effect of the inertia of the fluctuations on the average film motion and the average film thickness;
- influence of these fluctuations on a single drop impact, splash conditions on the outcome.

The case of direct drop interactions on the wall are considered in the studies (Roisman et al., 2002a; Roisman and Tropea, 2002).

In Section 3 the first attempt to characterize the motion in the liquid film associated with the fluctuations of the dynamic pressure is presented. This effect becomes especially important for the case of impact of dense and high-velocity sprays, such as a Diesel injection spray. Note, that this description cannot be considered as an exact model for such fluctuations, but more as an estimation for the characteristic velocity, length and time scales.

The theoretical predictions are validated by the comparison with the experimental data for the secondary spray Section 4. The conclusions are presented in Section 5.

2. Motion of a liquid film initiated by drop impacts

A necessary element in the understanding and modelling of spray impact is the hydrodynamics of the flow in a liquid film on a solid substrate. Each impacting drop disturbs the film motion. However, if the spray is relatively sparse, it is always possible to choose an area of the wall surface in which no drop impacts occur during some definite time period. The motion of the film during this time period is directed tangential to the wall surface and is governed mainly by inertial effects.

The theory of the flow in the film is given in Yarin and Weiss (1995) for the axisymmetric case and is generalized in Roisman and Tropea (2002) for the case of a two-dimensional plane film. The continuity equation of the film can be given in the following form:

$$\frac{\mathrm{D}h}{\mathrm{D}t} + h(\nabla \cdot \vec{V}) = 0 \tag{1}$$

where h is the film thickness, $\vec{V}$ is the average velocity vector over the film thickness and parallel to the wall, ∇ is the two-dimensional gradient operator in the plane parallel to the wall and $\mathrm{D}/\mathrm{D}t$ is the material time derivative.

If the gradient of the film thickness is small ($|\nabla h| \ll 1$) and if the motion in the film is produced by high Re and high We number impacts, such that the capillary and viscosity effects are negligibly small, the momentum balance in the plane parallel to the wall can be written in dimensionless form as

$$\frac{\mathrm{D}\vec{V}}{\mathrm{D}t} = 0 \tag{2}$$

Note that Eqs. (1) and (2) are valid only for the time period during which no drop impacts onto the considered element of the wall surface. This is the reason why the volume flux and the momentum associated with the drop impact events are not considered here.

The general solution of the governing equations (1) and (2) can be given in the Lagrangian form (Roisman and Tropea, 2002)

$$\vec{V} = \vec{V}_0(\vec{\zeta}), \quad \vec{x} = \vec{V}_0(\vec{\zeta})t + \vec{\zeta}, \quad h(\vec{\zeta}) = \frac{h_0(\vec{\zeta})}{1 + (\nabla_\zeta \cdot \vec{V}_0)t + \det(\nabla_\zeta \vec{V}_0)t^2} \tag{3}$$

where $\vec{x}$ is the radius vector of a material point initially located at $\vec{\zeta}$, $\vec{V}_0(\vec{\zeta})$ and $h_0(\vec{\zeta})$ are the initial velocity vector and the initial film thickness at the radius vector $\vec{\zeta}$, $\nabla_\zeta = \partial/\partial\vec{\zeta}$ is the gradient operator at the initial instant of time.

It can be easily shown that if $\det(\nabla_\zeta \vec{V}_0)$ is positive, the denominator in the right-hand side of the third equation (3) vanishes at some positive instant in time. In this case the solution produces a "kinematic discontinuity" (Yarin and Weiss, 1995; Roisman and Tropea, 2002) leading to the formation of an uprising sheet.

At this kinematic discontinuity (or at the "base of the sheet") the velocity in the film jumps from $\vec{V}_1(\vec{x},t)$ to $\vec{V}_2(\vec{x},t)$ and the film thickness jumps from $h_1(\vec{x},t)$ to $h_2(\vec{x},t)$ (see Fig. 6). The

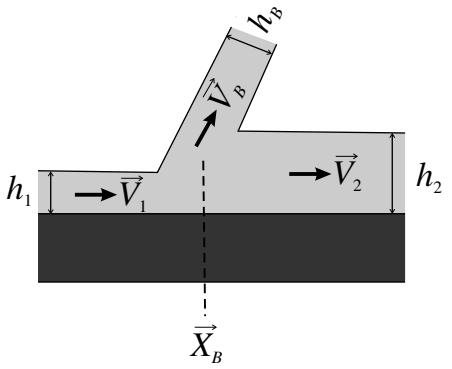

Fig. 6. Sketch of the uprising sheet at the wall.

position of the kinematic discontinuity is denoted in parametric form as $\vec{X}_{\mathrm{B}}(\xi, t)$, where ξ is a position parameter. Considering the mass, the momentum balance at the kinematic discontinuity and using the Bernoulli equation in the system moving with this base yields the equations of motion for the base of the sheet as well as the velocity and the thickness, $\vec{V}_{\mathrm{B}}$ and h_{B}, of the uprising sheet on the substrate

$$\frac{\partial \vec{X}_{\mathrm{B}}}{\partial t} = \frac{\vec{V}_1 + \vec{V}_2}{2} \tag{4}$$

$$\vec{V}_{\mathrm{B}} = \frac{\vec{V}_1 h_1 + \vec{V}_2 h_2}{h_1 + h_2} + |\vec{V}_1 - \vec{V}_2| \frac{\sqrt{h_1 h_2}}{h_1 + h_2} \vec{e}_z \tag{5}$$

$$h_{\mathrm{B}} = h_1 + h_2 \tag{6}$$

The above equations are valid for the high inertia (high Reynolds, high Weber numbers) flows in the relatively thin films. They can be used for the description of the sheets produced by the single drop impact into a liquid film or drop interactions on the wall.

2.1. Single drop impact onto a stationary uniform film

In Roisman and Tropea (2002) two main cases of single drop impact were described: normal impact onto a steady uniform film and normal impact onto a moving film. These descriptions include the expressions for the motion of the base of the uprising jet; for the velocity, thickness and the shape of this jet; for the position of the rim. Consider a Cartesian coordinate system $\{\vec{e}_x, \vec{e}_y, \vec{e}_z\}$, fixed at the wall surface, with the base vector $\vec{e}_z$ normal to the wall. Consider an inclined impact onto a steady uniform liquid film of thickness h_f of a single drop of the initial diameter D_0 and the impact velocity $U_n(-\vec{e}_z + \tan\theta \vec{e}_x)$. Here θ is the obliquity angle (between the drop velocity vector and the normal to the wall). This impacting drop creates a moving circular spot of radially expanding flow on the wall, whose velocity $\vec{V}_l$ and thickness h_l are written in dimensionless form as

$$\vec{V}_l = \frac{x\vec{e}_x + y\vec{e}_y}{t+\tau} + \tan\theta\,\vec{e}_x, \quad h_l = \frac{\eta}{(t+\tau)^2} \tag{7}$$

where U_n and D_0 are taken as the velocity and length scales, τ and η are constant parameters. It can be shown that expressions (7) correspond to the remote asymptotic solution of (3).

Using (7) in the expression (5) yields the following expressions for the base position of the sheet and for the velocity of the sheet ejected by the drop impact:

$$\vec{X}_{\mathrm{B}}(\varphi,t) = \left[\beta\cos\varphi + \tan\theta\left(\sqrt{(1+\tau)(t+\tau)} - \tau\right)\right]\vec{e}_x + \beta\sin\varphi\sqrt{t+\tau}\vec{e}_y \tag{8}$$

$$\vec{V}_{\mathrm{B}}(\varphi,t) = \frac{h_l}{h_l+h_f}\left[\frac{\vec{X}_{\mathrm{B}}}{t+\tau} + \frac{\tau\tan\theta}{t+\tau}\vec{e}_x + \sqrt{\frac{h_f(\beta^2 + 2\beta B\cos\varphi + B^2)}{h_l}}\vec{e}_z\right] \tag{9}$$

where β is a dimensionless parameter, $\varphi \in [-\pi,\pi]$ is the circumferential parameter, and $B = \tan\theta\sqrt{1+\tau}$. Expressions (8) and (9) are similar to the corresponding expressions obtained in (Roisman and Tropea, 2002) for the shape of the kinematic discontinuity and the velocity of the jet after the normal wall impact of a single drop into a uniform moving film. One important issue of oblique impact is the part of the kinematic discontinuity, $\varphi \in [-\varphi^*,\varphi^*]$, corresponding to the positive flux in the uprising sheet, where $\varphi^* = \arccos(-\beta/B)$. In other words, if $\beta > B$ the base of the crown is a closed curve, whereas if $\beta < B$ the sheet is ejected only from a part of the circle $\vec{X}_{\mathrm{B}}$ bounded by $\pm\varphi^*$.

2.2. Bending stability of a free rim, fingering and splash

A free liquid sheet, including our uprising sheets, are bounded by a rim. This free rim is formed due to capillary forces. The velocity of the rim differs from the velocity of the sheet, such that the inertia of the liquid entering the rim is balanced by surface tension. The velocity of the rim bounding a stationary, uniform liquid sheet was obtained by (Taylor, 1959) in the form

$$U_{\mathrm{R}} = \sqrt{\frac{2\sigma}{\rho h_{\mathrm{R}}}} \tag{10}$$

where h_{R} is the sheet thickness at the rim location.

As a result of this relative velocity, the rim first rises above the wall; when the sheet velocity is larger than U_{R}, it reaches a maximum height; then it collapses (when the sheet velocity is smaller than U_{R}), and falls back onto the wall.

In some cases (when the impact velocity exceeds the splashing threshold) the rim centerline deforms, giving rise to several finger-like jets. These jets then break up creating a number of secondary droplets.

The drops are formed at the end of each finger. The nature of these drops is exactly the same as the mechanism of the rim formation at the edge of a free sheet. The velocity of such drop is smaller than the velocity in the finger-like jet. Let us approximate the finger by a cylindrical jet of the diameter d_{F} and consider the momentum balance of the drop. This momentum equation describes

the balance of the inertia of the liquid entering the drop, capillary forces and the pressure p_σ in the jet:

$$\frac{\pi d_{\mathrm{F}}^2}{4}\rho U_{\mathrm{D}}^2 + \pi d_{\mathrm{F}}\sigma - p_\sigma \frac{\pi d_{\mathrm{F}}^2}{4} = 0 \tag{11}$$

where U_{D} is the jet velocity relative to the drop, and the pressure associated with the capillary effects is $p_\sigma = 2\sigma/d_{\mathrm{F}}$. The solution of Eq. (11) for the drop relative velocity is

$$U_{\mathrm{D}} = \sqrt{\frac{2\sigma}{\rho d_{\mathrm{F}}}} \tag{12}$$

The expression (12) determines the initial velocity of secondary droplets produced by the splash if the velocity of the jets is known. In the case of high Reynolds and low Froude impact of a single drop the acceleration of a material particle in the ejected sheet is negligibly small (Roisman and Tropea, 2002; Peregrine, 1981), the velocity of the fingers is thus known and equal to the ejection velocity (9).

In Yarin and Weiss (1995) the mechanism of cusp formation and fingering is proposed based on the assumption that the rim propagates with the constant velocity U_{R}. They have shown how the initial rim disturbance is transformed from a smooth curve to the "broken" line. In (Roisman and Tropea, 2002) the instant of the cusp formation, when the radius of the curvature of the rim centerline vanishes, is estimated as a function of the initial curvature radius.

However, this mechanism is not able to explain the initial growth of the rim disturbances leading to the typical crown-like shape of the sheets obtained by drop impacts. One important parameter which was not taken into account in the previous studies of the rim stability and break-up is the velocity gradient in the free sheet. To illustrate the effect of the velocity gradient, let us consider the cartesian coordinate system x', y' in the plane of the sheet (see Fig. 7). The origin of this coordinate system is fixed at the rim $x' = 0$, and the y'-axis is directed along the rim centerline. The liquid in the sheet $x' < 0$ moves with the velocity $u = U_{\mathrm{R}}$. Consider now small disturbances of the rim centerline: $\delta(y', t)$ and the velocity gradient $\gamma = \partial u/\partial x'$ in the sheet. The linearized equation for the growth of the disturbances is

$$\frac{\partial \delta}{\partial t} = \gamma \delta \tag{13}$$

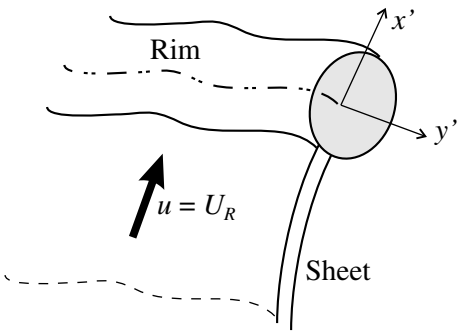

Fig. 7. Sketch of the rim bounding a sheet.

the solution of which for the constant γ is $\delta = \exp(\gamma t)$. Therefore, the rim centerline is always stable if the velocity gradient $\gamma < 0$ and unstable when $\gamma > 0$. It should be noted here that the importance of the velocity gradient in the rim break-up mechanism was independently understood by Rieber (2003).

The velocity of the ejected sheet produced by drop impact, determined in (9), decreases with time. Therefore, the spatial velocity gradient $\partial u/\partial x'$ in the sheet is positive and the bending disturbances rim are unstable. The splash thus takes place when the time for the cusp formation, rim fingering and break-up of the fingers is shorter than the time of the rim uprising and falling onto the wall.

The theoretical model for the velocities of the secondary droplets, developed in this section, is validated by comparison with the data for polydisperse water spray impact. These results are discussed in Section 4.

3. Typical scales of film fluctuations on the wall

3.1. Main assumptions and definitions

Consider the impact of a dense spray onto a flat, horizontal, rigid substrate. We assume that the thickness of a liquid film created on the substrate is much smaller than both the characteristic size of the spray and the characteristic size of the target. The first assumption allows one to substitute the parameters of the spray at the fluctuating film surface by the corresponding parameters at the stationary wall surface. The second assumption yields $|\nabla_w h| \ll 1$, where h is the film thickness, such that the long-wave approximation can be applied to equations of film motion. Following this approximation, $|\nabla_w| \ll \partial/\partial z$ and the main flow is directed parallel to the wall, where z is the coordinate normal to the wall.

Consider also the long-time behavior of spray impact using the assumption $\partial/\partial t = 0$ in the time-averaged equations of motion of the film. Note, that this long-time behavior differs from a steady state because the time-dependent fluctuations are accounted for in the modelling.

As an example, we consider the simplest case of a uniform normal spray impact with the drops velocity defined as $\vec{v} = -u\vec{e}_z$, where the unit normal vector $\vec{e}_z$ is directed against the main stream of the primary spray.

The local volume, number and momentum flux densities (Roisman and Tropea, 2000) at the wall surface are given in the form

$$\vec{q} \equiv \frac{\pi c_n(\vec{x},t)}{6}\int_{-\infty}^{\infty}\int_{0}^{\infty} D^3\vec{v}f(\vec{x},t,\vec{v},D)\,\mathrm{d}D\,\mathrm{d}v_z = -\dot{q}\vec{e}_z \tag{14}$$

$$\vec{n} \equiv c_n(\vec{x},t)\int_{-\infty}^{\infty}\int_{0}^{\infty} \vec{v}f(\vec{x},t,\vec{v},D)\,\mathrm{d}D\,\mathrm{d}v_z = -\dot{n}\vec{e}_z \tag{15}$$

$$\dot{\mathbf{P}} \equiv \frac{\rho\pi c_n(\vec{x},t)}{6}\int_{-\infty}^{\infty}\int_{0}^{\infty} D^3\vec{v}\otimes\vec{v}f(\vec{x},t,\vec{v},D)\,\mathrm{d}D\,\mathrm{d}v_z = \dot{P}\vec{e}_z\otimes\vec{e}_z \tag{16}$$

where $c_n(\vec{x},t)$ is the number concentration of droplets in the spray, $f(\vec{x},t,\vec{v},D)$ is the probability density function, $\dot{q}$, $\dot{n}$ and $\dot{P}$ are positive constants. $\dot{P}$ is actually the average "dynamic pressure" produced by the spay. The geometry of the considered problem is axisymmetric.

The flow in the film produced by spray impact is influenced by the inertia of the velocity fluctuations. These fluctuations appear due to single drop impacts. The phenomenon of a single drop impact onto a stationary uniform liquid layer is studied intensively experimentally (Harlow and Shannon, 1967; Levin and Hobbs, 1971; Macklin and Metaxas, 1976; Cossali et al., 1997) with one of the main aims being to develop a model of spray impact (Bai et al., 2002; Mundo et al., 1998; Tropea and Roisman, 2000). Recent theoretical studies of (Yarin and Weiss, 1995; Trujillo and Lee, 2001) allows one to describe the flow produced by drop impact, the crown propagation or even the interaction of two crowns (Roisman and Tropea, 2002).

It is possible to determine a number of characteristic scales describing a single drop impact. The usual scales are the initial diameter, D_0, as a length scale and the normal impact velocity, U_0, as a velocity scale, and D_0/U_0 as a time scale. In the case of the train of drops produced by the drop generator (Yarin and Weiss, 1995) an additional time scale, $1/f$, can be introduced, where f is the frequency of drop impact. The length scale characterizing the spray transport is $c_n^{-1/3}$, where c_n is the number concentration of the droplets in the spray. This characteristic length scale can be associated with the average distance between the droplets in the spray. However, it is impossible to determine either the length scale or the time scale characterizing the polydisperse spray impact directly from the given spray parameters.

Below is a model allowing one to estimate such scales from the balance of the inertial term in the spray and in the fluctuating liquid layer.

3.2. Distribution of impacts around a given drop impact: fluctuating pressure

Consider the impact of very dense, uniform spray such that the viscous and capillary effects can be neglected in comparison to the inertia of the liquid. The velocity field $\vec{u}$ in the liquid can be subdivided into two parts: a time-averaged part $\bar{\vec{u}}$ and a fluctuating part $\vec{u}'$, and can be presented in the form $\vec{u} = \bar{\vec{u}} + \vec{u}'$. Note, that part $\vec{u}'$ of the velocity field is associated with the fluctuations produced by the single drop impacting onto the liquid boundary, whereas the part $\bar{\vec{u}}$ is time-averaged over the time comparable with the characteristic time of the spray. This means that $\bar{\vec{u}}$ is constant for the steady spray and not constant for intermittent spray impact. In the analysis below only a steady spray is considered and all the time-averaged values besides velocity are independent on time.

Assume for simplicity that the time-averaged velocity $\bar{\vec{u}}$ in the film vanishes and the time-averaged parameters of the spray are uniform. This situation is true near the center of symmetry of the target, $r \to 0$. Assume also axial symmetry around the axis $\vec{e}_z$, such that $\vec{u}'_s = u'_s\vec{e}_r$. The subscript s means that the velocity is associated with a single drop impact.

The time-averaged pressure in the film is $\dot{P}$, which is assumed to be constant in our example, $\partial\dot{P}/\partial r = 0$. However, the temporal and spatial fluctuations of this pressure, $p'_s(r,t)$, play a role of a driving force producing the flow fluctuations in the film.

In this case the radial component of the momentum balance equation for the fluctuating part of the flow on the wall can be written in the form

$$\frac{\partial h}{\partial t}+\frac{1}{r}\frac{\partial(rhu_s')}{\partial r}=0, \tag{17}$$

$$\frac{\partial(rhu_s')}{\partial t}+\frac{\partial(rhu_s'^2)}{\partial r}=-\frac{rh}{\rho}\frac{\partial p_s'}{\partial r}. \tag{18}$$

We will not consider the deterministic distribution of the pressure p_s' produced by the drop impacts around the given drop D_0. However, we consider the statistically averaged pressure p_s' produced by these impacts.

The average number of drops (including drop D_0) impacting onto a circle of radius r during the time interval t after impact is $\lambda=\pi r^2 t\dot{n}$, where the constant number flux density into the film is defined as $\dot{n}=-\vec{n}\cdot\vec{e}_z$. What is the distribution of drops around our drop D_0? Intuitively, when we remove one drop from the uniformly distributed drops, we will obtain a "hole" in the neighborhood of the location of this removed drop. It is obvious that if $\lambda\gg 1$ the average number of drops around the drop D_0 is $\lambda_1\approx\lambda-1$. Below is the exact analysis of the drop distribution around the drop D_0 for any λ.

Assuming that the drops of the spray are distributed randomly in space and in time, the probability $\mathscr{P}(k,\lambda)$ that exactly k drops impact onto the considered circle can be described by the Poisson distribution (Feller, 1968):

$$\mathscr{P}(k,\lambda)=\frac{\mathrm{e}^{-\lambda}\lambda^k}{k!}. \tag{19}$$

The latter assumption is valid even in the relatively close proximity to the nozzle of water spray, as was shown experimentally using the phase Doppler instrument (Roisman and Tropea, 2000).

In order to determine the distribution $\mathscr{P}_1$ of drops around the given drop D_0, the case $k=0$ with the probability $\mathscr{P}(0,\lambda)=\mathrm{e}^{-\lambda}$ should be excluded from the set of possible events. The minimum possible k number is 1 (because the drop D_0 has already hypothetically impacted onto the considered area). Thus, the distribution $\mathscr{P}_1$ can be given with the help of (19) by

$$\mathscr{P}_1(k_1,\lambda)=\frac{\mathrm{e}^{-\lambda}\lambda^{k_1+1}}{(1-\mathrm{e}^{-\lambda})(k_1+1)!}, \tag{20}$$

where $k_1=k-1$ is the number of drops impacted into the circle, excluding the drop D_0. The term $(1-\mathrm{e}^{-\lambda})$, which is the probability that at least one drop including D_0 will impact onto the circle, appears in the denominator of the expression for $\mathscr{P}_1$ as a normalization parameter.

The expressions for the probabilities $\mathscr{P}$ and $\mathscr{P}_1$ are similar but different. However, this does not mean that other drops in the spray "know" about the impact of the drop D_0. These probabilities describe very different events. The probability distribution $\mathscr{P}$ describes random impacts of all the impacting drops, whereas the distribution $\mathscr{P}_1$ describes the impacts of drops except the drop D_0 which, we know, have already impacted onto a wall.

The average number of drops impacting onto the circle around the given point D_0 is

$$\lambda_1(r,t)=\sum_{k_1=0}^{\infty}k_1\mathscr{P}_1=\lambda\mathrm{e}^{\lambda}\xi^{-1}-1 \tag{21}$$

where $\xi = e^{\lambda} - 1$. This number depends on the radius of the considered area around the drop D_0 and the time.

On the other hand, the number of drops λ_1 can be determined using the statistically averaged number flux density $\dot{n}_1(r,t)$ of the drops around the drop D_0:

$$\lambda_1 = \int_0^t \int_0^r 2\pi r \dot{n}_1(r,t)\,\mathrm{d}r\,\mathrm{d}t \tag{22}$$

The expressions (21) and (22) are used to determine $\dot{n}_1(r,t)$ in the form $\dot{n}_1(r,t) = G(r,t)\dot{n}$ where

$$G(r,t) = \frac{1}{2\pi r \dot{n}} \frac{\partial^2 \lambda_1}{\partial t \partial r} = e^{\lambda}[\xi^{-1} - 3\lambda\xi^{-2} + (2+\xi)\lambda^2\xi^{-3}] \tag{23}$$

The function G expresses the ratio of the statistically averaged number flux $\dot{n}_1$ of drops around the given drop D_0 to the constant number flux $\dot{n}$. This function approaches unity in the limit $\lambda \to \infty$. This means that the average distribution of the drops far from D_0 is not influenced by the drop impact.

A variation of G in the radial direction means that the statistically averaged pressure $p_s' = G\dot{P}$ applied by the surrounding drops also varies, causing flow fluctuations in the film. This statistically averaged flow will be analyzed below.

Using the length scale Λ, the time scale T and the velocity scale Υ in the form

$$\Lambda = \left[\frac{\dot{P}}{\dot{n}^2\pi^2\rho}\right]^{1/6}, \quad T = \left[\frac{\rho}{\dot{P}\dot{n}\pi}\right]^{1/3}, \quad \Upsilon = \frac{\Lambda}{\mathrm{T}} \tag{24}$$

the equation for the statistically averaged mass balance and the momentum in the radial direction can be obtained using the Eqs. (18) in dimensionless form

$$\frac{\partial \tilde{h}}{\partial \tilde{t}} + \frac{1}{\tilde{r}} \frac{\partial(\tilde{r}\tilde{h}\tilde{u}_s')}{\partial \tilde{r}} = 0, \tag{25}$$

$$\frac{\partial \tilde{u}_s'}{\partial \tilde{t}} + \tilde{u}_s' \frac{\partial \tilde{u}_s'}{\partial \tilde{r}} = -\frac{\partial G}{\partial \tilde{r}}, \tag{26}$$

where the variables with tilde are dimensionless, with Λ and T being used as length and time scales. The parameter λ can be written using the new dimensionless variables as $\lambda = \tilde{r}^2\tilde{t}$.

Consider first the approximate solution of equations (25) and (26) as $r \to 0$. The linearized right-hand side of (26) obtained from (23) is

$$\frac{\partial G}{\partial \tilde{r}} \approx \frac{2}{3} rt$$

and the approximate solution of (25) and (26) solved for the velocity of fluctuations and the film thickness, subject the initial conditions

$$\tilde{h} = \tilde{h}_0 = const, \quad \tilde{u}_s' = 0, \quad \text{at } \tilde{t} = 0,$$

is

$$\tilde{u}_s' = -\tilde{r}\tilde{t}^2/3 \frac{{}_0F_1(;5/3;-2\tilde{t}^3/27)}{{}_0F_1(;2/3;-2\tilde{t}^3/27)}, \quad \tilde{h} = \tilde{h}_0\,{}_0F_1(;2/3;-2\tilde{t}^3/27)^{-2}$$

where ${}_0F_1(;a;b)$ is the hypergeometric function. It can be shown that this solution becomes singular near the axis $\tilde{r} = 0$ at the time instant $\tilde{t}^* \approx 2.274$. This instant corresponds to the kinematic discontinuity in the velocity gradient (''shock'') causing the creation of an uprising central jet. This phenomena was observed in the experiments with the Diesel spray impact (see Fig. 5). Also, such jets not associated with any crown produced by a single drop impact were observed even during not so ''aggressive'' water spray impact (Tropea and Roisman, 2000; Sivakumar and Tropea, 2002). The nature of such a kinematic discontinuity is very similar to the process leading to the formation of the uprising crown-like sheets produced by the single drop impact (Yarin and Weiss, 1995), inclined sheets produced by the oblique drop impact (Roisman and Tropea, 2002) or drop interactions on the substrate (Roisman et al., 2002a).

Consider again the system of non-linearized differential equations (25) and (26). The numerical solution of this system, valid for all the radii, obtained using the expression (23) for the function G is shown in Figs. 8 and 9. The velocity distribution $\tilde{u}'_s$ in the film is shown in Fig. 8. As the time approaches the critical value $\tilde{t}^* = 2.274$ the velocity gradient at the center ($\tilde{r} = 0$) goes to minus infinity, whereas the film thickness grows infinitely (see Fig. 9). Note however, that our model for the flow of fluctuations is based on the long-wave approximation of flow in the thin film is not valid for times $\tilde{t} > \tilde{t}^*$ and is not developed to describe the flow in the central jet. The flow in this jet is mostly longitudinal, normal to the wall, leading to the jet stretching. Moreover, at the end of the jet, an almost spherical droplet is formed due to the capillary forces. The motion of this drop determines the length of the jet, which is in reality finite.

It is convenient to define the average velocity, $\langle v_z \rangle$, and average diameter, $\langle D \rangle$, of the spray in the form

$$\langle v_z \rangle = \frac{\dot{P}}{\rho \dot{q}}, \quad \langle D \rangle = \left[\frac{6\dot{q}}{\pi \dot{n}}\right]^{1/3} \tag{27}$$

where the parameters corresponding to the ''dynamic pressure'', $\dot{P}$, and the volume flux, $\dot{q}$, are defined in (16) and (14).

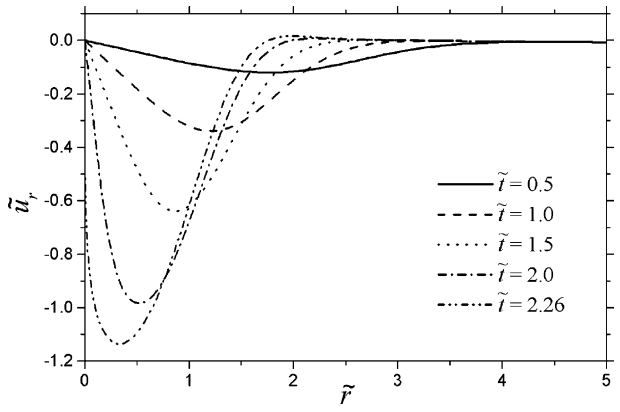

Fig. 8. The dimensionless, statistically averaged radial velocity $\tilde{u}_r$ in the film.

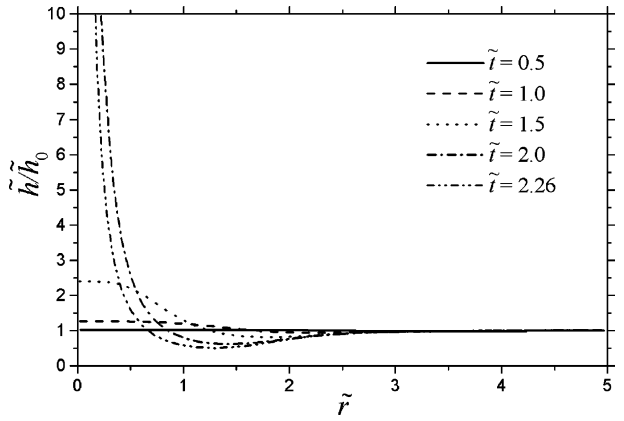

Fig. 9. The dimensionless, statistically averaged thickness $\tilde{h}$ of the film.

The expressions for the scales (24) yield

$$\Lambda = \langle D \rangle \left[\frac{\langle v_z \rangle}{36\dot{q}} \right]^{1/6}, \quad T = \frac{\langle D \rangle}{\left[6\dot{q}^2 \langle v_z \rangle \right]^{1/3}}, \quad \Upsilon = \left[\dot{q} \langle v_z \rangle \right]^{1/2} \tag{28}$$

4. Results and discussion

In order to validate the model presented in Section 2, measurements of the drop diameter and two components of the velocity were performed in a water spray using the phase Doppler technique. The detection volume was located 1 mm above a metal polished target. The sign of the u-component of the drop velocity was used to distinguish droplets before impact ($u > 0$) from secondary droplets ($u < 0$). The spray was produced using a commercial pressure swirl atomizer. The parameters of the spray were varied, changing the distance of the nozzle from the impact target, atomization pressure, volume flux, type of the nozzle, and impingement angle.

In Fig. 10 examples of the velocity distributions of drops are shown: the measured velocity vector on the left-hand side, and the theoretical predictions on the right-hand side. The gray level in the contour plot is proportional to the logarithm of the probability density function $f(u, v)$, where v is the transverse (parallel to the wall) component of the velocity vector. The simulations are based on Eq. (9) for the velocity of the uprising sheet. The tangential velocity V_τ vanishes since the impact is normal.

The parameters β, τ and η are estimated from the initial conditions. It is assumed that the duration of the initial drop deformation is of order D_0/U_n. The thickness of the initial spot produced by the drop is assumed to be equal to the undisturbed film thickness (Yarin and Weiss, 1995) and the energy loss during this period is neglected. The values of the parameters τ and η are obtained in (Roisman and Tropea, 2002) in the following form:

$$\beta = \left(\frac{3h_f}{2} \right)^{-1/4}, \quad \tau = \frac{1}{\sqrt{24h_f}} - 1, \quad \eta = \frac{1}{24} \tag{29}$$

(h_f being the dimensionless initial thickness of the film).

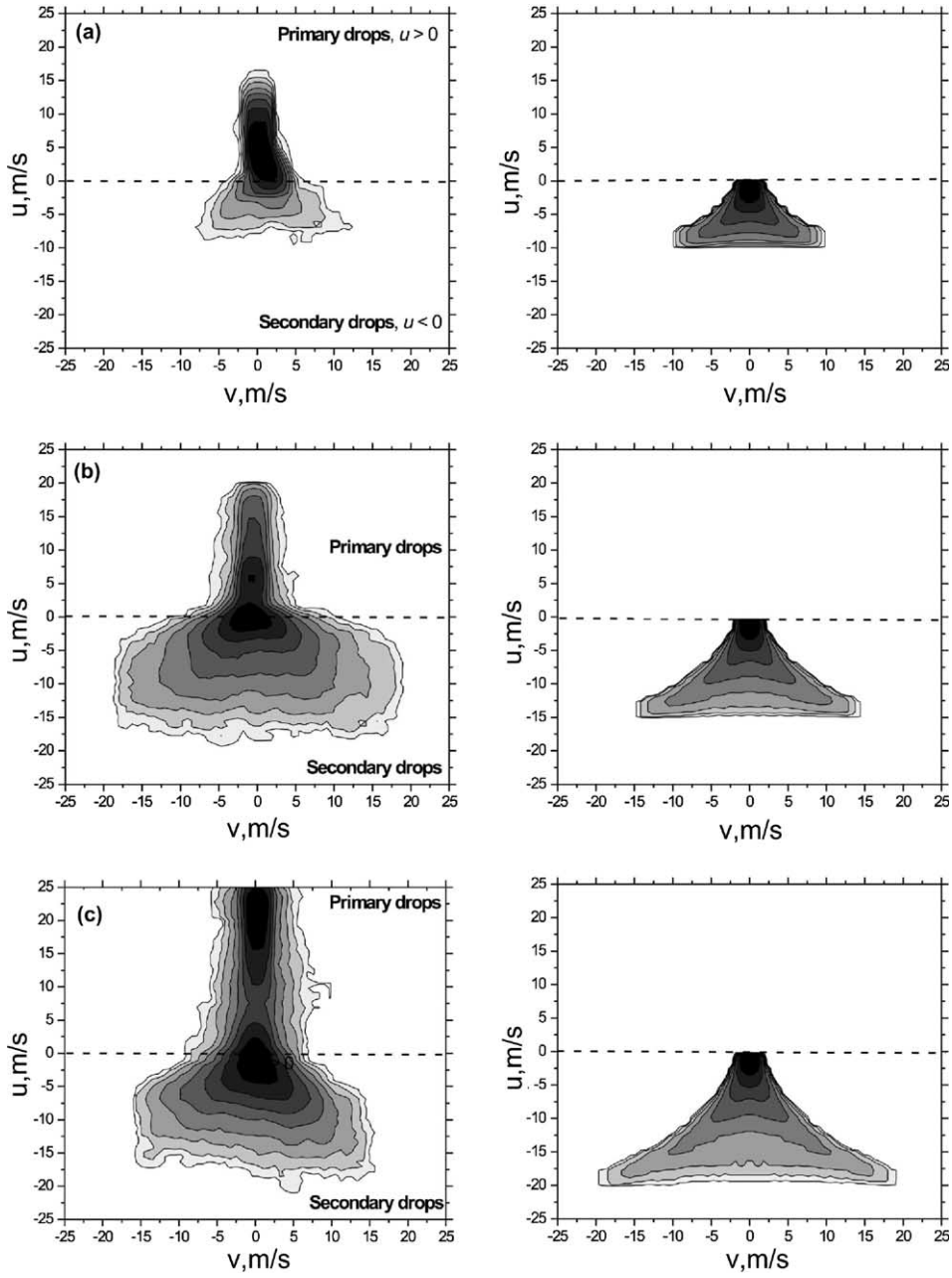

Fig. 10. Normal impact of a water spray. Comparison of experimental data for the velocity distribution (left) with the theoretical prediction for the secondary spray (right). The impact velocity used for simulations is: (a) $U_0 = 10$ m/s; (b) $U_0 = 15$ m/s and (c) $U_0 = 20$ m/s.

The direction of the motion of the secondary droplets coincides with the direction of $\vec{V}_B$ from (9), although the magnitude is smaller by the value of the relative drop velocity, determined with

the help of expression (12). This relative velocity is estimated assuming the diameter of the jet to be of the same order as the diameter (~40 μm) of the secondary droplets (known from the measurements). For the given conditions this relative velocity is approximately 2 m/s. In the three cases shown in Fig. 10 the impact velocity for the simulations was chosen from the measurement data as an average velocity of droplets before impact exceeding the splashing threshold $We^{4/5}Re^{2/5} \geqslant 2800$ (Tropea and Roisman, 2000).

The experimental data shown in Fig. 10 includes both primary ($u > 0$) and secondary ($u < 0$) droplets. The average velocity of the primary droplets from the experiment, exceeding the splashing threshold $We^{4/5}Re^{2/5} \geqslant 2800$ (Tropea and Roisman, 2000), is calculated and used in (9) to determine the distribution of the secondary droplets. This distribution of the secondary droplets is shown on the right side of Fig. 10. Therefore, only the negative values of the droplet velocity should be considered when comparing the theory with the data.

In all the cases the predicted velocity distribution is of the same order as the measured velocity distribution. The wider and smoother "cloud" depicting the measured velocities can be associated with the interaction between droplets, which is not accounted for in the present simulations. Note, that the characteristic velocity of film fluctuations determined in (28) is much smaller than the droplet velocity in these relatively sparse sprays. Their influence on the velocity of the secondary droplets is neglected.

The case of inclined impact of water spray is shown in Fig. 11. The velocity distribution in this case is very different from the normal spray impact. The velocities of the secondary droplets after normal impact are directed in all directions, whereas the velocities after an inclined impact are directed mainly in one direction. However, as shown in Fig. 11b, this can be explained within the framework of the crown splash and described using equations (9) and (12). The hydrodynamics of inclined drop impact onto a liquid film depends significantly on the impact angle (Roisman and Tropea, 2002). A frequently applied hypothesis is the use of a critical $We_n^{4/5}Re_n^{2/5}$ number, where We_n and Re_n are the Weber and Reynolds numbers based on the normal component of the drop velocity. Using such approach, our experiments lead to the result that no splash occurs, because all the parameters of all the primary drops are below the assumed critical number $We_n^{4/5}Re_n^{2/5} = 2800$.

We do not discuss the splash threshold models in the present work. The dependence of the number of the secondary droplets as a function of the impact conditions is also not modelled in the present work, a topic of on-going research in several groups. The most probable velocity of the primary drops in the experiments shown in Fig. 11(a) is $7.5\vec{e}_z + 6.3\vec{e}_x$ m/s. In Fig. 11(b) the results of the theoretical predictions of the velocity distribution of the secondary droplets produced by such impact are shown. These results agree well with the data for the secondary droplets ($u < 0$) shown in Fig. 11(a). Two additional simulations are shown in Fig. 11(b) and (c) in order to demonstrate the sensitivity of the model to the impact parameters. The normal, u-components of the impact velocity, $u = 9.7$ m/s and $u = 12.4$ m/s, are the average velocities of the primary drops from the data, whose tangential impact velocity is $v = 8$ m/s and $v = 10$ m/s, respectively.

The theory overpredicts the values for the velocities in cases shown in Fig. 11(b) and (c). However, the main direction of the predicted secondary velocities is predicted well in all the considered cases.

The example of the very dense Diesel spray impact is shown in Fig. 12. In this contour plot the experimental data for the velocity distribution in the spray is depicted. The impact velocity ranges

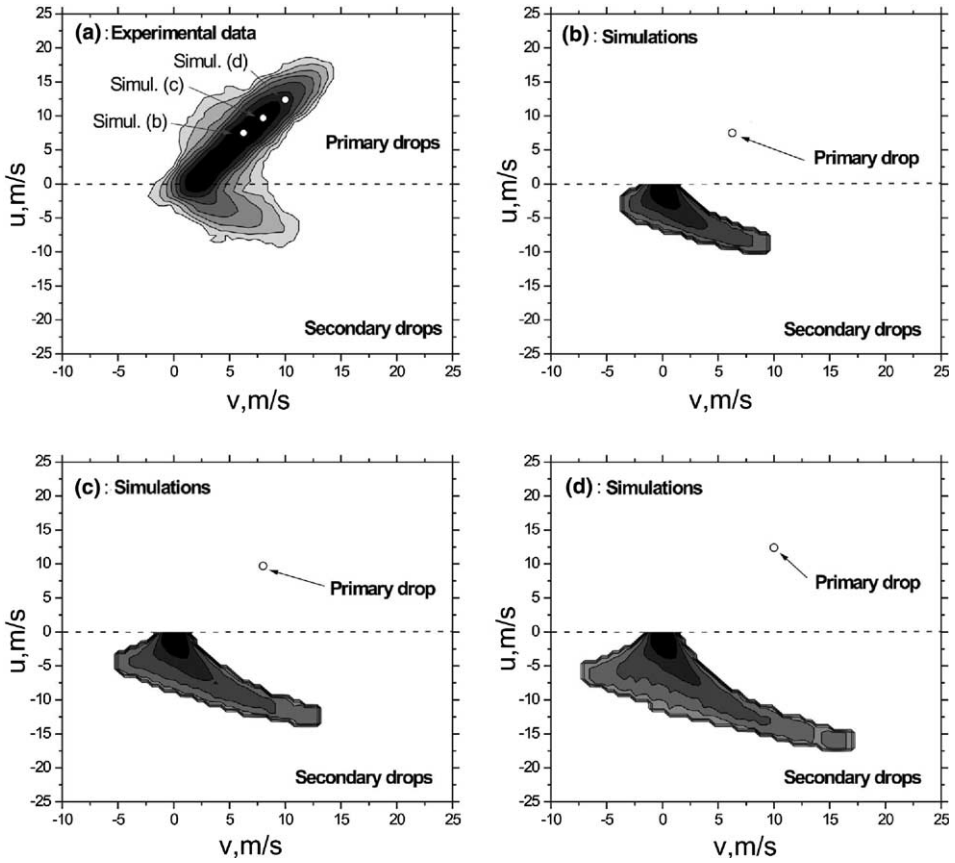

Fig. 11. Inclined impact of a water spray. Comparison of experimental data for the velocity distribution: (a) with the theoretical prediction for the secondary spray. The impact velocities used for the simulations are: (b) $u = 7.5$ m/s, $v = 6.3$ m/s and (c) $u = 9.7$ m/s, $v = 8$ m/s; (d): $u = 12.45$ m/s, $v = 10$ m/s. The parameters of primary drops used for the simulations are shown also in (a) as white circles.

from zero to almost 70 m/s, whereas the magnitude of the velocity of the secondary droplets is smaller than 10 m/s. The simulations based on expressions (9) and (12) overpredict the magnitude of the velocity of the secondary droplets significantly. We do not show here these results because these secondary droplets are not created as the result of the crown splash and Eqs. (9) and (12) are not appropriate. As was noted in Section 1, the Diesel spray is so dense that there is not sufficient place for crowns to expand.

The model for the interaction of the impacted drops on the wall (Roisman et al., 2002a; Roisman and Tropea, 2002) yields even higher values for the predicted velocity of the secondary drops and also cannot be applied to the description of diesel spray impact.

The small secondary drops can be created only by the break-up of finger-like jets (or by a chaotic explosive disintegration, which is definitely not our case). In the case of a low-velocity, sparse spray, or impact of a single drop, these jets appear after the break-up of crown-like uprising sheets. In the case of dense diesel spray impact, we didn't observe any crowns. The only jets we have observed are single and appear directly from the film.

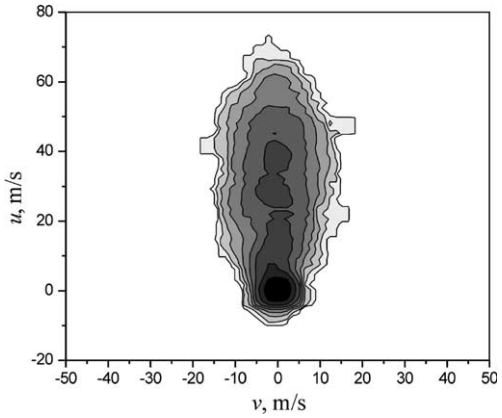

Fig. 12. Normal impact of a dense diesel spray. Experimental data for the distribution of the velocity of droplets.

In the present study we check the hypothesis that these jets can be associated with the fluctuations of the dynamic pressure. The diameter of the secondary drops is of order of the characteristic size of film fluctuations, whereas their velocity magnitude is of the order of the characteristic velocity of such fluctuations.

The value of the average local volume flux density $\dot{q}$ is estimated by simply measuring the volume of the injected and collected fuel over a defined time. This value is of order 0.2 m/s at an injection pressure of 150 bar, and 0.3 m/s at an injection pressure of 300 bar. The values of $\dot{q}$ is used in equations (28) to determine the values for the scales of the film fluctuations. In Figs. 13 and 14 the average drop diameter, D_a, and the magnitude of the average normal velocity, U_a, of the secondary spray produced by the Diesel spray impact are shown as functions of Λ and Υ, determined for various spray parameters. It is shown that both the predicted length scale of the film fluctuations and predicted velocity scale are of the same order as the D_a and U_a. Moreover, D_a and U_a correlate well with Λ and Υ, respectively. This represents therefore a qualitative validation of the model presented in Section 3.

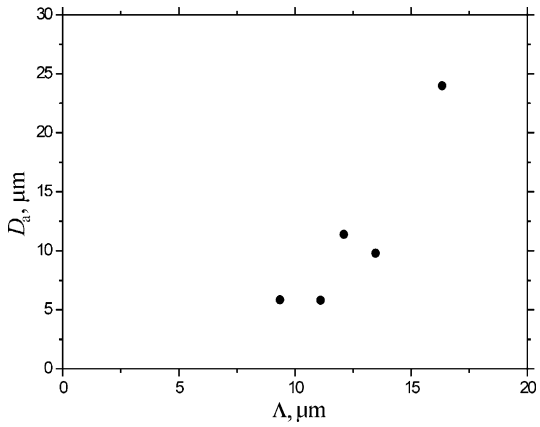

Fig. 13. Normal impact of a dense diesel spray. Average diameter of the secondary droplets as a function of the length scale for the film fluctuations Λ.

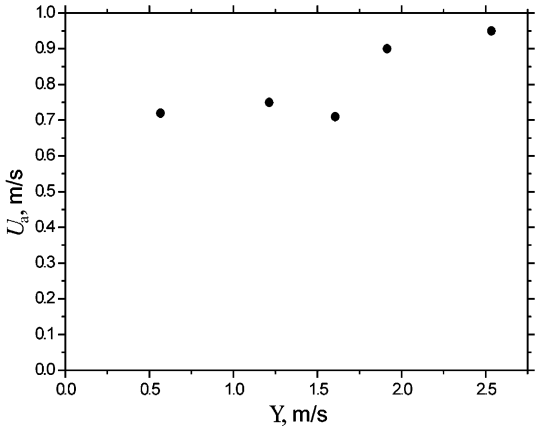

Fig. 14. Normal impact of a dense diesel spray. Average normal velocity of the secondary droplets as a function of the velocity scale for the film fluctuations Υ.

5. Conclusions

In the present paper the hydrodynamics of a liquid film produced by an impinging spray as well as the velocity of the secondary spray are considered. The spray is described as a continuum, exhibiting specific properties, such as number concentration of particles and their probability density function. Particulary, two asymptotic cases of spray impact are considered: very spare spray impact characterized by small relative crown presence (Tropea and Roisman, 2000), such that the effect of their interaction can be neglected; and very dense spray impact.

The fluctuations in the liquid film on the wall influence the splashing threshold, even in the case of the relatively spare spray. Nevertheless, the velocities of the secondary droplets produced by the wall impact of such sparse spray can be described by the model of normal or oblique crown ejection. The agreement between theory and experiment is very encouraging. This agreement indicates that the inertial effects associated with drop impacts are the dominant factor in formation of the uprising sheets, whereas the capillary forces influence the velocity of the secondary droplets.

This model, based on the single drop impact, is not valid in the case of very dense Diesel spray impact when the characteristic velocity Υ of film fluctuations determines the velocity of secondary droplets, and the characteristic length Λ determines their diameter.

The paper explains the emergence of the liquid jets during the impact of very dense sprays through fluctuations of the pressure. The short times are considered during which the pressure produced by the impacting drops can no longer be considered continuous over the wall surface. Moreover, the characteristic time, length and velocity of these fluctuations are determined in terms of integral parameters of the impacting spray. It is shown that the velocity of secondary droplets produced by very dense Diesel spray impact are of the same order as the value of estimated characteristic velocity of film fluctuations, Υ, and the average diameter of these secondary droplets is of order of the characteristic length Λ of fluctuations.

Note that in Section 3 the normal impact of a steady uniform spray is analyzed. However, this model can be applied even to the highly unsteady and not uniform sprays (as for example Diesel injection spray) if the characteristic size Λ of the film fluctuations is much smaller that the typical

size of the spray and if the characteristic time T of these fluctuations is much smaller that the typical time associated with the change of spray characteristics with time.

References

Bai, C., Rusche, H., Gosman, A.D., 2002. Modeling of gasoline spray impingement. Atomizat. Sprays 12, 1–27.
Cossali, G.E., Coghe, A., Marengo, M., 1997. The impact of a single drop on a wetted surface. Exp. Fluids 22, 463–472.
Feller, W., 1968. An Introduction to Probability Theory and its Applications, vol. I, third ed. John Wiley & Sons, New York, Chichester, Brisbane, Toronto.
Harlow, H., Shannon, J.P., 1967. The splash of a liquid drop. J. Appl. Phys. 38, 3855–3866.
Levin, Z., Hobbs, P.V., 1971. Splashing of water drops on solid and wetted surfaces: hydrodynamics and charge separation. Philos. Trans. R. Soc. Lond. A 269, 555–585.
Macklin, W.C., Metaxas, G.J., 1976. Splashing of drops on liquid layers. J. Appl. Phys. 47, 3963–3970.
Mundo, C., Sommerfeld, M., Tropea, C., 1998. On the modelling of liquid sprays impinging on surfaces. Atomizat. Sprays 8, 625–652.
Oğuz, H.N., Prosperetti, A., 1990. Bubble entrainment by the impact of drops on liquid surfaces. J. Fluid Mech. 219, 143–179.
Peregrine, D.H., 1981. The fascination of fluid mechanics. J. Fluid Mech. 106, 59–80.
Rieber, M., 2003. Private communication.
Rioboo, R., Marengo, M., Tropea, C., 2000. Outcomes from a drop impact on solid surfaces. Atomizat. Sprays 11, 155–165.
Roisman, I.V., Prunet-Foch, B., Tropea, C., Vignes-Adler, M., 2002a. Multiple drop impact onto a dry solid substrate. J. Colloid Interface Sci. 256, 396–410.
Roisman, I.V., Rioboo, R., Tropea, C., 2002b. Normal impact of a liquid drop on a dry surface: model for spreading and receding. Proc. R. Soc. London A 458, 1411–1430.
Roisman, I.V., Tropea, C., 2000. Flux measurements in sprays using phase doppler techniques. Atomizat. Sprays 11, 673–705.
Roisman, I.V., Tropea, C., 2002. Impact of a drop onto a wetted wall: description of crown formation and propagation. J. Fluid Mech. 472, 373–397.
Sivakumar, D., Tropea, C., 2002. Splashing impact of a spray onto a liquid film. Phys. Fluids Lett. 14, L85–L88.
Stanton, D.W., Rutland, C.J., 1998. Multi-dimensional modeling of thin liquid films and spray–wall interactions resulting from impinging sprays. Int. J. Heat Mass. Tran. 41, 3037–3054.
Taylor, G.I., 1959. The dynamics of thin sheets of fluid. II. waves on fluid sheets. Proc. R. Soc. London A 263, 296–312.
Tropea, C., Roisman, I.V., 2000. Modelling of spray impact on solid surfaces. Atomizat. Sprays 10, 387–408.
Trujillo, M.F., Lee, C.F., 2001. Modeling crown formation due to the splashing of a droplet. Phys. Fluids 13, 2503–2516.
Yarin, A.L., Weiss, D.A., 1995. Impact of drops on solid surfaces: self-similar capillary waves, and splashing as a new type of kinematic discontinuity. J. Fluid Mech. 283, 141–173.